

Added Figures:

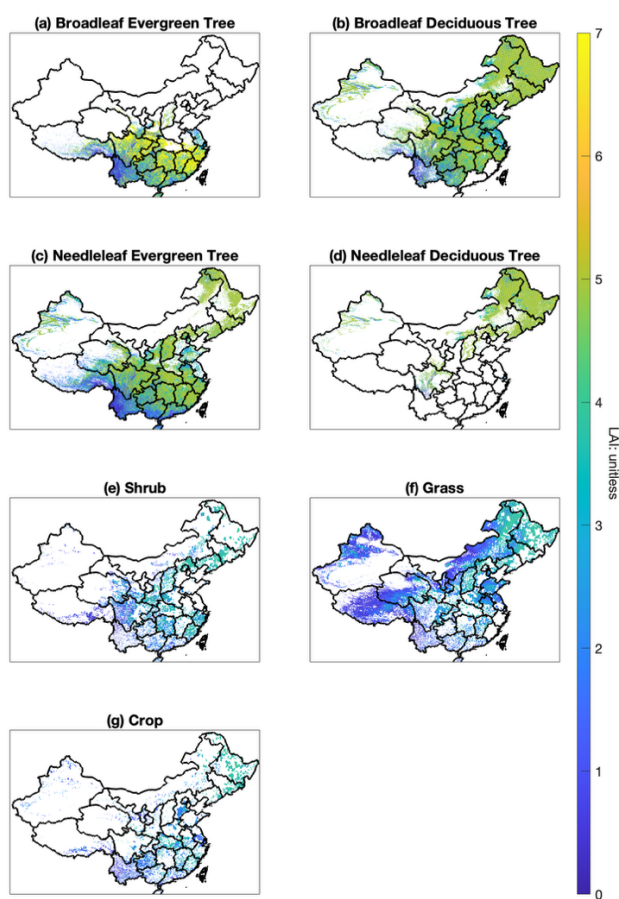


Figure S1. PFT-specific leaf area index (LAI) distributions of the MR approach for July 2013, representing peak summer conditions when isoprene emissions are maximum.

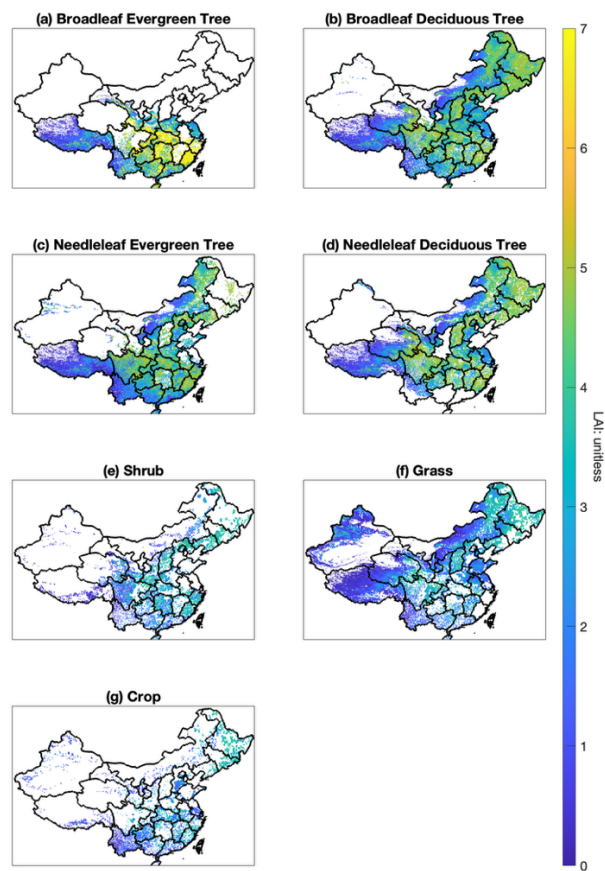


Figure S2. PFT-specific leaf area index (LAI) distributions of the HR approach for July 2013, representing peak summer conditions when isoprene emissions are maximum.

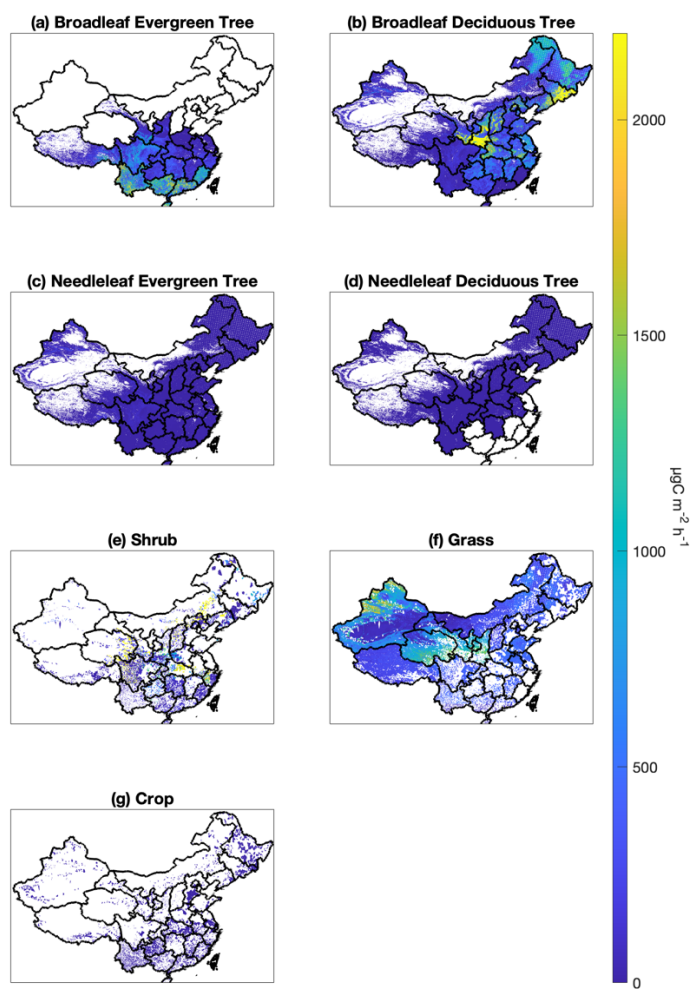


Figure S3. Combined emission factor and PFT fraction products ($\text{EF} \times \text{fraction}$) for the MR approach, representing the emission potential per unit area for each vegetation type.

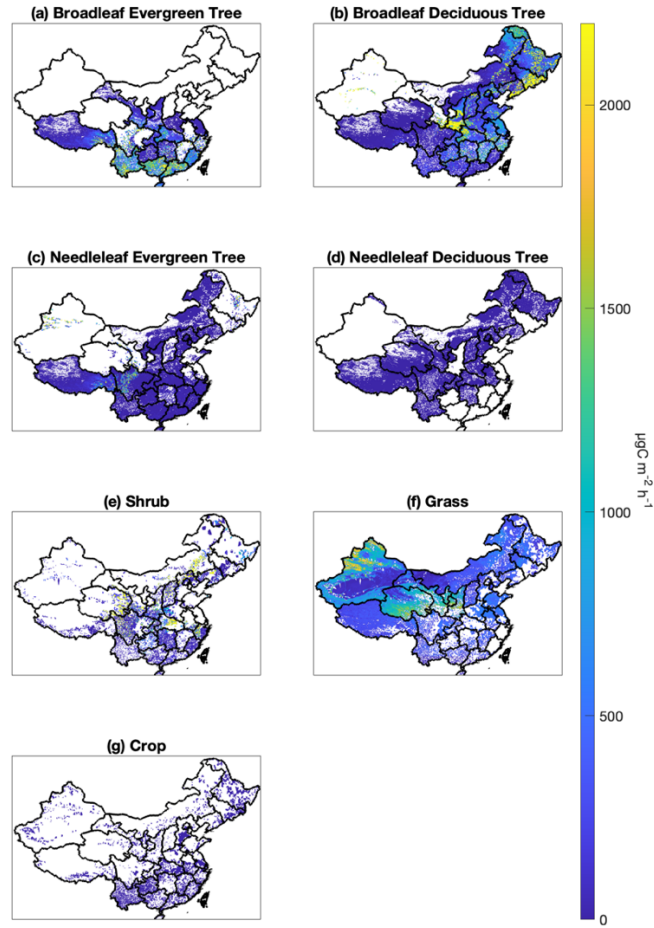


Figure S4. Combined emission factor and PFT fraction products ($\text{EF} \times \text{fraction}$) for the HR approach, representing the emission potential per unit area for each vegetation type.

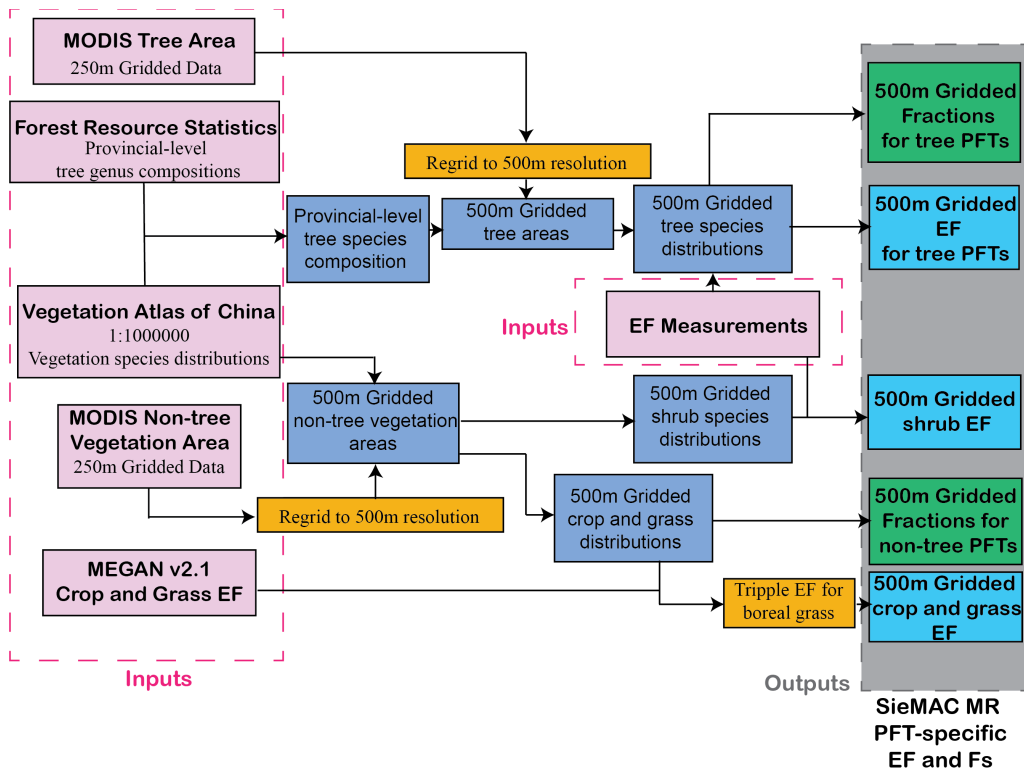


Figure S5. Data integration workflow for the MR approach, showing the integration of Forest Resource Statistics, Vegetation Atlas, and MODIS products.

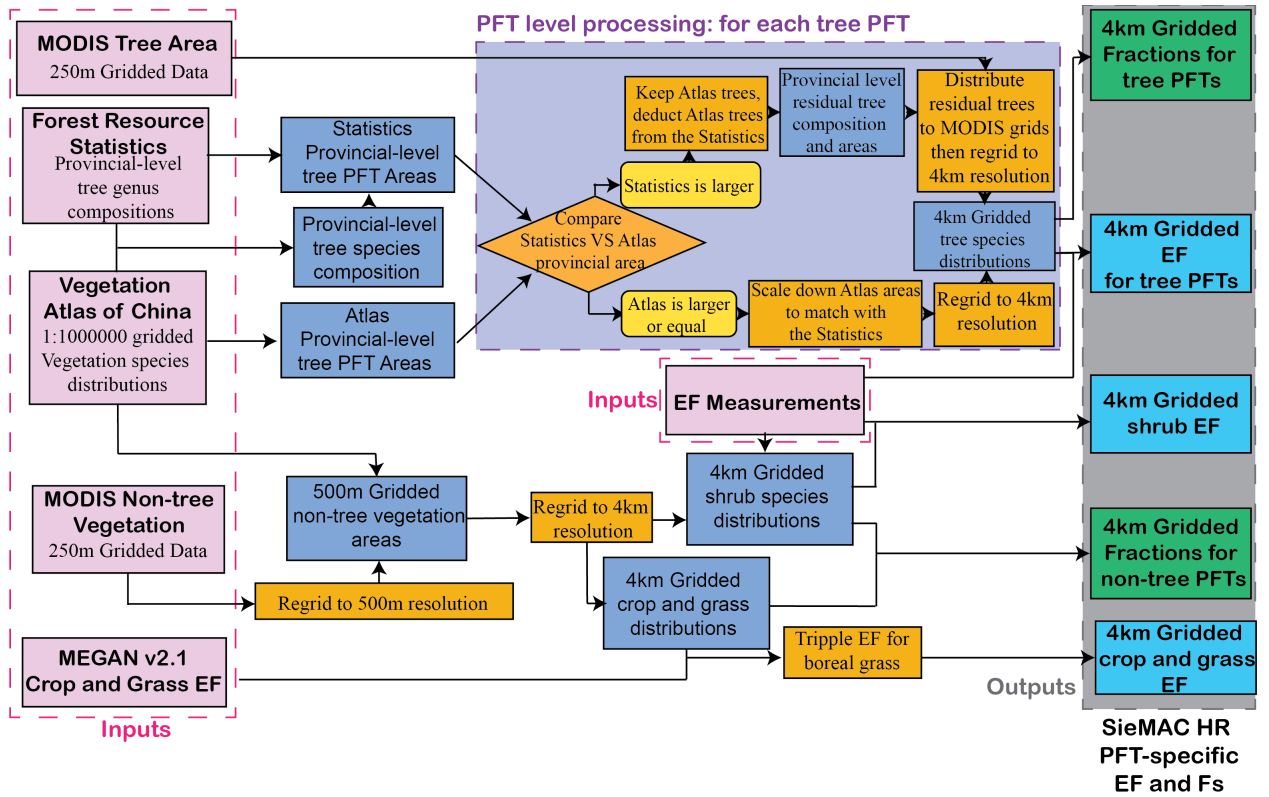


Figure S6. Data integration workflow for the HR approach, showing the MODIS-based methodology with simplified data requirements.

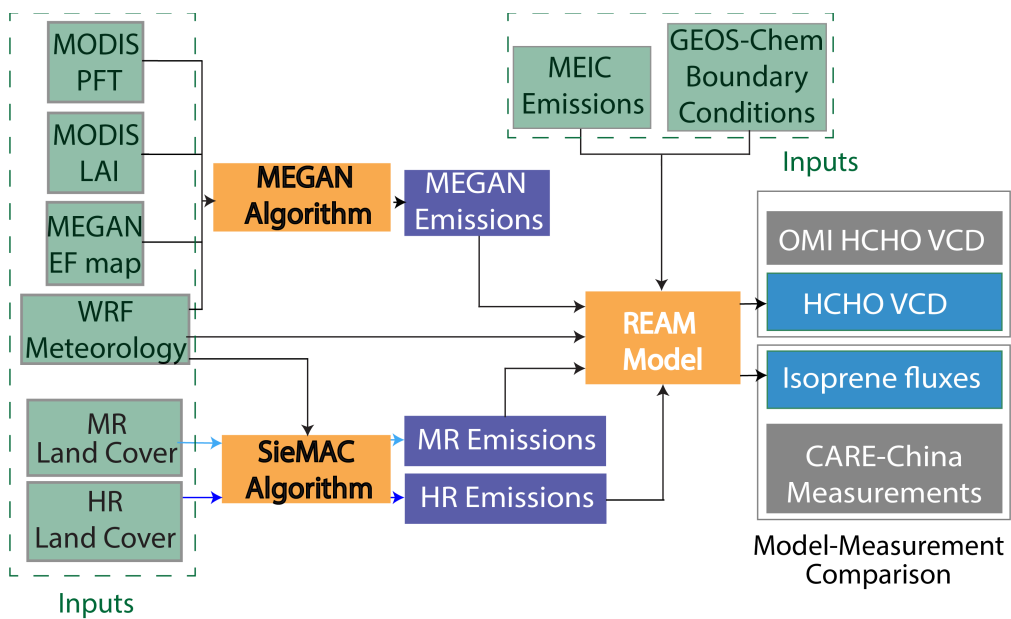
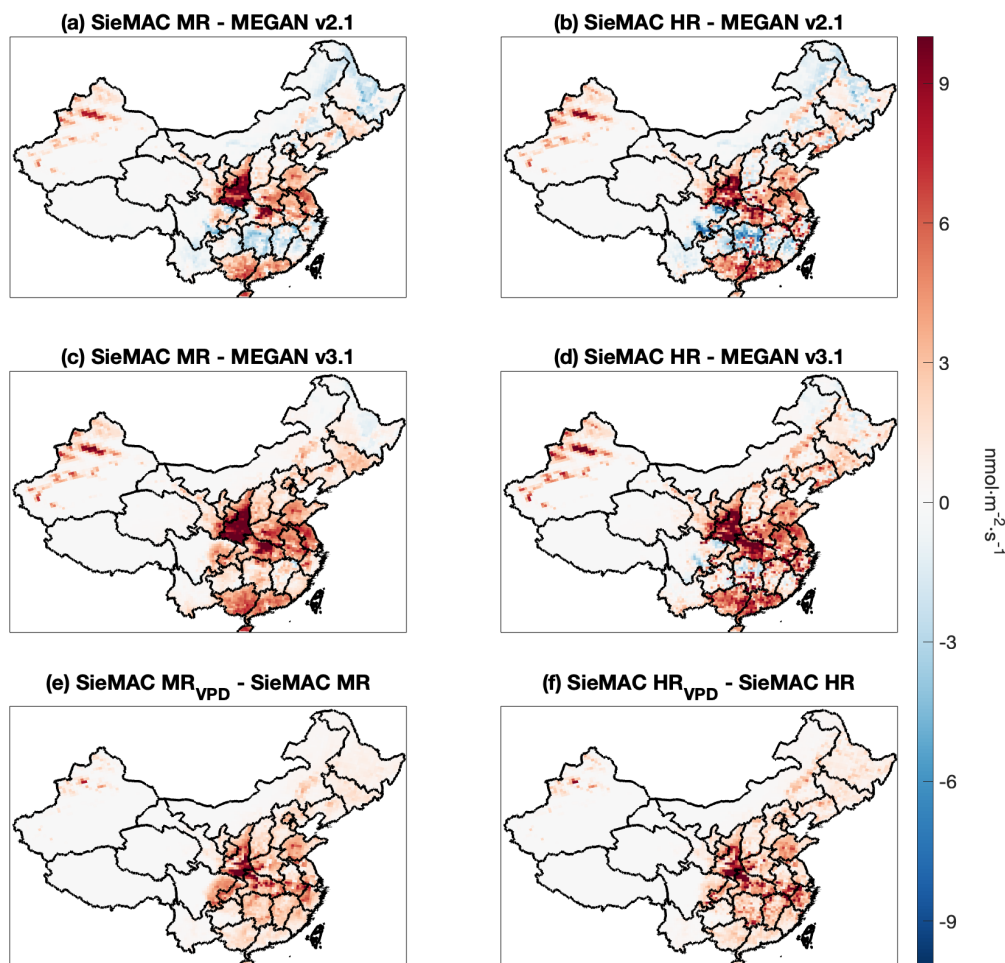
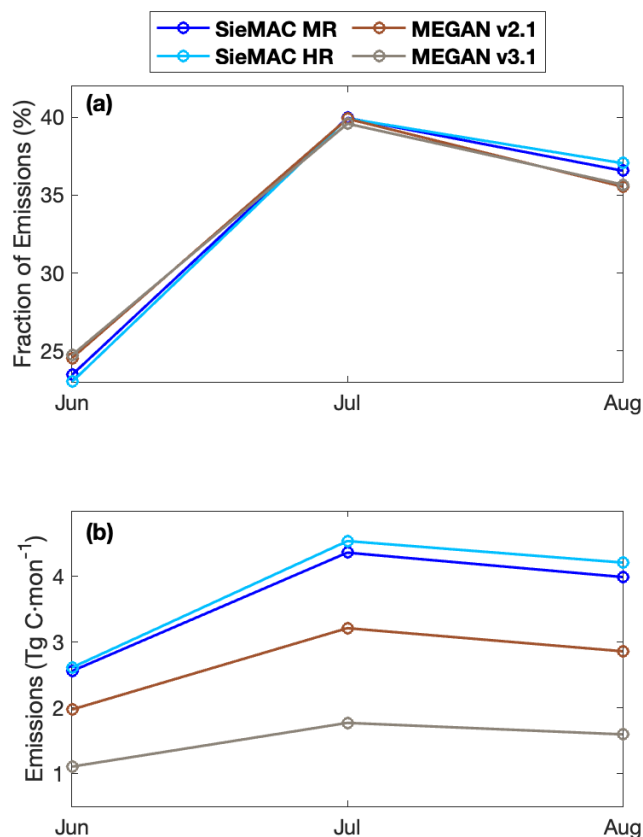


Figure S7. Schematic diagram of the REAM model setup showing the integration of SieMAC isoprene emissions and evaluation against observational datasets.

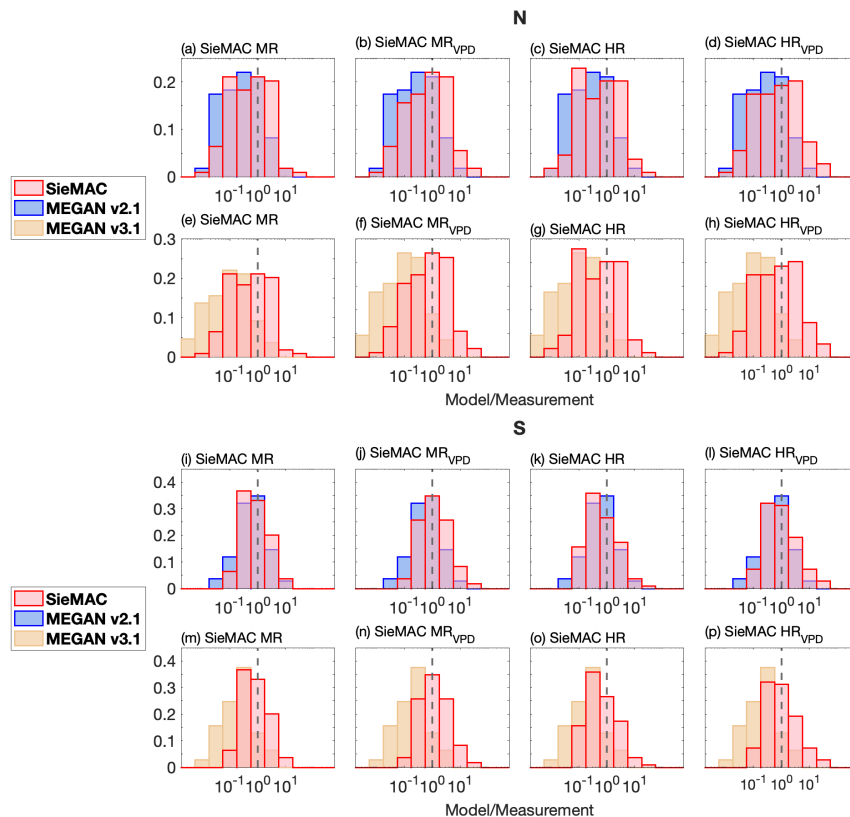
Revised Figures:



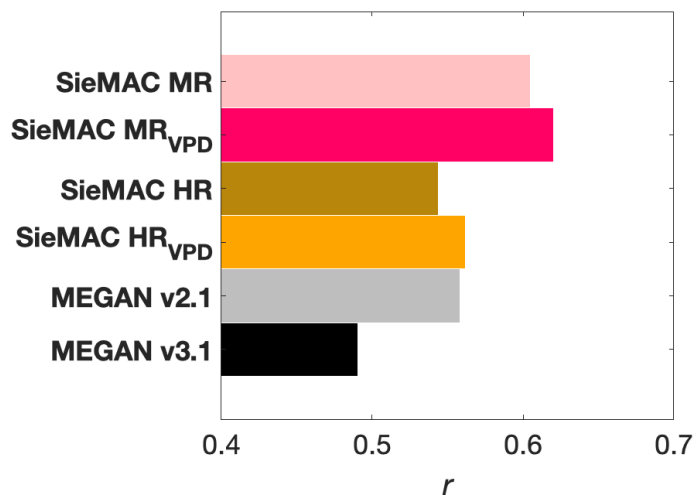
Revised Figure 9. Spatial differences in isoprene emissions (summer 2013) among different schemes. (a) and (b) map the difference between SieMAC and MEGAN v2.1 for MR and HR, respectively (SieMAC – MEGAN v2.1). (c) and (d) map the difference between SieMAC and MEGAN v3.1 for MR and HR, respectively (SieMAC – MEGAN v3.1). (e) and (f) quantify the impact of vapour pressure deficit stress by subtracting the unstressed SieMAC fields from their VPD-enabled counterparts (SieMAC MR_{VPD} – SieMAC MR and SieMAC HR_{VPD} – SieMAC HR). Colours denote the magnitude of the difference in nmol m⁻² s⁻¹ (scale at right); red shades indicate higher emissions in the first-listed inventory, while blue shades indicate lower emissions.



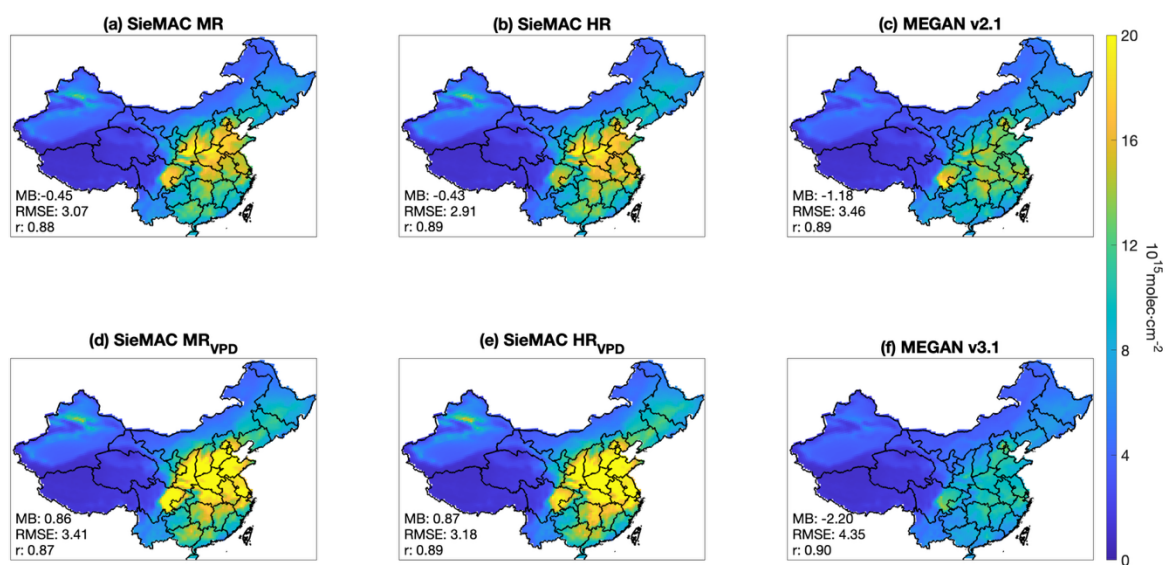
Revised Figure 11. Monthly variation of isoprene emissions for summer 2013 in four inventories: SieMAC MR (dark blue), SieMAC HR (light blue), MEGAN v2.1 (brown), and MEGAN v3.1 (grey). (a) shows the relative monthly emissions expressed as a percentage of each inventory's total summer emission, permitting direct comparison of seasonal progression across inventories. (b) presents absolute monthly emissions in Tg C mon^{-1} , showing the magnitude differences between emission inventories.



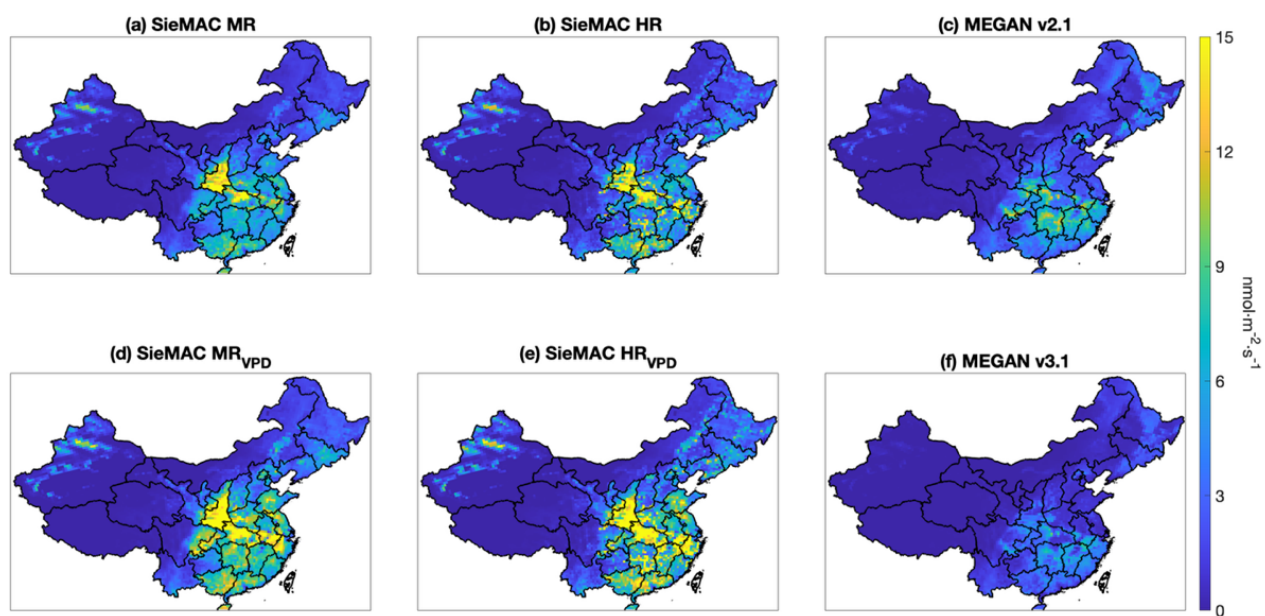
Revised Figure 5. Distributions of the model-to-measurement ratio for surface isoprene at CARE-China sites. Histograms are shown separately for northern (N, panels a–h) and southern (S, panels i–p) regions. Within each region, the four columns, from left to right, correspond to the SieMAC configurations: MR, MR_{VPD}, HR, and HR_{VPD}. Red bins represent SieMAC results, blue bins represent MEGAN v2.1, and yellow bins represent MEGAN v3.1. The x-axis is logarithmic with a bin width of 0.5. The vertical dashed line marks the 1:1 ratio.



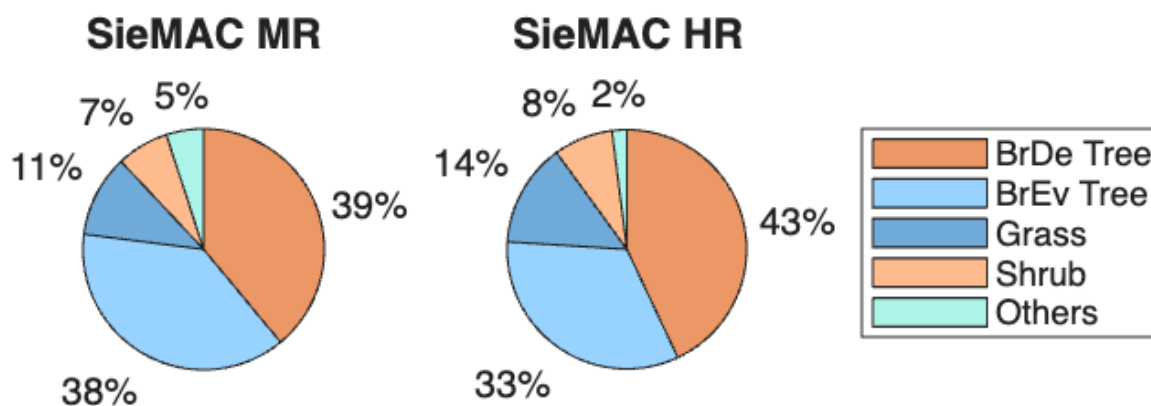
Revised Figure 6. Spatial correspondence between modelled isoprene emissions and satellite formaldehyde (HCHO). Bars give the Pearson correlation coefficient (r) between grid-cell seasonal mean isoprene emission from each inventory—SieMAC MR, SieMAC MR_{VPD}, SieMAC HR, SieMAC HR_{VPD}, MEGAN v2.1, and MEGAN v3.1—and Ozone Monitoring Instrument (OMI) HCHO vertical column over mainland China for summer 2013. Higher values of r indicate a closer match in the spatial patterns of isoprene emissions and observed formaldehyde.



Revised Figure 7. Seasonal mean of formaldehyde (HCHO) vertical columns (VC) for summer 2013 simulated with six emission inventories. (a) SieMAC MR, (b) SieMAC HR, (c) MEGAN v2.1, (d) SieMAC MR_{VPD}, (e) SieMAC HR_{VPD}, and (f) MEGAN v3.1. Values are expressed in $10^{15} \text{ molec cm}^{-2}$. Statistics in the lower-left corner of each panel give the mean bias (MB), the root-mean-square error (RMSE), and Pearson spatial correlation coefficient (r) between model and OMI HCHO VCs across all grid cells, quantifying the overall amplitude and spatial agreement with observations.



Revised Figure 8. Summertime (2013) isoprene emissions over mainland China derived from six emission schemes: (a) SieMAC MR, (b) SieMAC HR, (c) MEGAN v2.1, (d) SieMAC MR_{VPD}, (e) SieMAC HR_{VPD}, and (f) MEGAN v3.1. Shade shows emission rate in $\text{nmol m}^{-2} \text{s}^{-1}$ (colour scale at right).



Revised Figure 10. Relative contribution of each PFT to the total isoprene emissions during summer 2013, shown separately for MR (a) and HR (b). BrDe Tree and BrEv Tree refer to broadleaf deciduous and broadleaf evergreen trees, respectively; "Others" comprises needleleaf trees and crops. Values next to each sector give the percentage contribution to the total national emissions attributable to that PFT.